Mon. Not. R. Astron. Soc. **000**, 1–5 (2014) Printed 20 August 2014 (MN LATEX style file v2.2)

The ratio of pattern speeds in double-barred galaxies

Joan Font[1⋆]John E. Beckman[1,2,3], Javier Zaragoza-Cardiel[1,2], Kambiz Fathi[4,5], Benoit Epinat[6,7], Philippe Amram[6,7]

[1] *Instituto de Astrofísica de Canarias, c/ Vía Láctea s/n, E38205, La Laguna, Tenerife, Spain*
[2] *Departamento de Astrofísica. Universidad de La Laguna, Tenerife, Spain*
[3] *Consejo Superior de Investigaciones Cientficas, Spain*
[4] *Department of Astronomy, Stockholm University, AlbaNova Center, 106 91 Stockholm, Sweden*
[5] *Oskar Klein Centre for Cosmoparticle Physics, Stockholm University, 106 91 Stockholm, Sweden*
[6] *Laboratoire dAstrophysique de Marseille, Université dAix-Marseille. Marseille. France*
[7] *CNRS, UMR7326, 38, rue F. Juliot-Curie, 13388 Marseille Cedex 13, France*

arXiv:1408.4274v1 [astro-ph.GA] 19 Aug 2014

Draft 20 August 2014

ABSTRACT

We have obtained two-dimensional velocity fields in the ionized gas of a set of 8 double-barred galaxies, at high spatial and spectral resolution, using their Hα emission fields measured with a scanning Fabry-Perot spectrometer. Using the technique by which phase reversals in the non-circular motion indicate a radius of corotation, taking advantage of the high angular and velocity resolution we have obtained the corotation radii and the pattern speeds of both the major bar and the small central bar in each of the galaxies; there are few such measurements in the literature. Our results show that the inner bar rotates more rapidly than the outer bar by a factor between 3.3 and 3.6.

Key words: Galaxies: structure; Galaxies: kinematics & dynamics; Galaxies: evolution

1 INTRODUCTION

The idea that nested bars could provide a mechanism for feeding the central massive black holes of galaxies dates from an article by Shlosman et al. (1989). It was understood that a major bar in a galaxy allows, via angular momentum exchange, gas to flow towards the center, but when this in gas reaches a galactocentric radius of some the half the bar width the gravitational asymmetry reaches virtually zero, so the mechanism is no longer effective. Shlosman et al. (1989) postulated that a small, nuclear bar within the main bar, offering an asymmetric field allows inflow to continue towards the nucleus. As observations increased in sensitivity, a significant fraction of barred galaxies was observed to harbour secondary nuclear bars, (see Erwin (2004, 2011)) although there may not be a preponderance of double barred galaxies among active galaxies (Erwin & Sparke 2002).

It is important to know whether nuclear bars are dynamically decoupled from the outer bar. Early simulation arguments (Shlosman et al. 1989; Pfenniger & Norman 1990) suggested that they should be decoupled and rotating faster than the outer bars. This received support from orbital models (Rautiainen & Salo 1999; Maciejewski & Sparke 2000; Rautiainen et al. 2002; Maciejewski & Athanassoula 2008) and N-body simulations (Rautiainen et al. 2002; Shen & Debattista 2009). Indirect evidence that the bars are decoupled is that that their relative position angles are randomly distributed (Buta & Crocker 1993; Erwin 2011). Models of individual galaxies where the gas morphology is derived from a potential model with two rotating bars also indicate that the two should rotate with different pattern speeds; e.g. NGC 4314 (Ann 2001) and NGC1068 (Emsellem et al. 2006). For the latter the authors used supporting kinematic measurements from a Sauron data cube.

There are few measurements in the literature of pattern speeds for nuclear bars in double-barred galaxies. Corsini et al. (2003) applied the Tremaine-Weinberg (TW) method (Tremaine & Weinberg 1984) to the stellar component of NGC 2950, showing that the two have different pattern speeds, although it was difficult to obtain a reliable value for the inner bar. Fathi et al. (2009) used the TW method on the Hα emission line velocity fields of 10 galaxies, finding evidence in three of them for a more rapidly rotating nuclear bar. As shown by Maciejewski & Singh (2008), the TW method may not give a true value for the inner pattern speed, but it can show that there is an inner component in rotation at a higher angular velocity than the outer component.

We have developed a new general method for finding corotation radii, and hence pattern speeds of resonant sys-

⋆ E-mail: jfont@iac.es

© 2014 RAS

tems in disc galaxies. This relies on measuring, at high enough angular and velocity resolution, the radii at which the non-circular velocity of the gas changes phase (Kalnajs 1978; Contopoulos & Papayannopoulos 1980). We use 2D velocity maps in Hα emission obtained with a Fabry-Perot spectrometer. This method requires sufficient star forming activity to produce widespread Hα, which allows us to measure late type disc galaxies. It was introduced in Font et al. (2011), applied to a sample of eight galaxies; in Font et al. (2014) we applied an improved version to 104 galaxies. The angular resolution available, in the range 0.8 - 4.4 arcsec, lets us find the corotations of nuclear bars as well as major bars and the spiral arm system. Here we have applied it to eight double barred galaxies.

In the next section we describe briefly the method, in section three we give the sources of our observations, and present our results, including analysis of the resonances in the individual galaxies; in section four we discuss our results.

2 THE STREAMING PHASE-REVERSAL METHOD

The principles of the method used were described in Font et al. (2014). Here we give a summary, to explain the guidelines of the technique. Using a Fabry-Perot data cube in Hα emission we derive a spectrum for each position on a galaxy, and transform it into 2D maps of integrated flux, l.o.s. velocity and velocity dispersion. Deriving the rotation curve from the velocity field and subtracting it off, in two dimensions, from the original map we get the map of the residual, non-circular (streaming) velocities. We effect the separation of circular and non-circular velocity over the full 2D field, using an iterative process to yield a non-axisymmetric field, which becomes the prime material for our method.

This residual velocity map is used to derive the phase reversal histogram (see figure 1). We locate those positions in the residual velocity field in which the streaming velocity changes sign when traced along the radial direction (a phase-reversal). To minimize noise and projection problems, a valid phase-reversal must satisfy two criteria, based on the angular and the velocity resolutions (Font et al. 2014). Plotting the radial distribution for the phase-reversals as a function of galactocentric radius we assign each of the maxima in this histogram to a resonance. From the rotation curve, we can derive the frequency curves $\Omega, \Omega \pm \kappa/2, \Omega \pm \kappa/4$, where Ω is the angular speed and κ the epicyclic frequency. These curves are used to classify the resonance as corotation, inner and outer Lindblad resonance (ILR, OLR), plus the ultraharmonic resonances (UHR), to study the couplings between the resonances, and to determine the pattern speeds. In Font et al. (2014) we found that most resonances for most of the galaxies are associated with corotations, with a small fraction of objects showing peaks which can be identified as ILRs or OLRs.

3 RESULTS

3.1 The observational data

The data set for three of the galaxies in our sample was the GHASP Fabry-Perot database (Epinat et al. 2008) taken on the 1.93m telescope at the Observatoire de Haute Provence. We selected those galaxies where we could see a double bar: a large outer bar and a small central bar. The galaxies chosen were: NGC 2595, NGC 5430 and NGC6946. The moment maps of these objects are available on the data base (Surace et al. 2009). The observational parameters for these objects: as pixel scale, angular and spectral resolution, and geometrical parameters (position angle, inclination and distance) can be found in (Epinat et al. 2008).

We take from the same data base, the first moment maps of NGC4321, NGC1097 and NGC4725, the first from the VIRGO survey (Chemin et al. 2006) using the FaNTOmM Fabry-Perot at the1.6m Mont Mgantic telescope, these authors also give the observational and geometrical paramters for this galaxy; the two remaining galaxies belong to the SINGS data base (Kennicutt et al. 2003); (Daigle et al. 2006; Dicaire et al. 2008) took the Fabry-Perot observations, respectively, at Mont Mgantic, The geometrical parameters for NGC 1097 can be found in Piñol-Ferrer et al. (2014), while the observational parameters for this galaxy together with all parameters of NGC 4725 are given in Daigle et al. (2006).

The data cubes for M61 (NGC 4303) and NGC 3504, obtained at the 4.2m William Herschel telescope, La Palma, with the GHαFaS Fabry-Perot instrument, show the highest angular resolution or "seeing" value (1.2 and 0.8 arcsec, respectively) and spectral sampling resolution (8.25 km$\cdot$s^{-1}) , and S:N ratio.

3.2 Corotations and associated resonance radii

In Figure 1 we show, for each galaxy, a histogram giving the radial dependence of the number of detected phase reversals. The vertical solid lines mark the radial positions of the maxima in the distributions, positively identified as resonances; the horizontal bars at the top show the uncertainty for each resonance. In the present study, we only consider the corotations associated with the two bars. To establish which of the resonances corresponds to the corotation of a given bar, we first apply the bar corotation (BC) criterion defined in Font et al. (2014): the strongest peak in the phase-reversal distribution located near the end of the bar is assumed to lie at its corotation. The position of this peak gives the bar corotation radius. When we find two or more peaks which satisfy the BC criterion we use the predictions by Rautiainen et al. (2008) who give, for the main bar, values for $\mathcal{R}$, the ratio of the corotation radius to the bar length as a function of morphological type, to decide which peak corresponds to the bar corotation radius. In each histogram of Figure 1, the corotations of the nuclear bar and of the outer bar are labeled as CR:Inner Bar and CR:Outer Bar, respectively. The dashed vertical lines show the lengths of the bars, given in Columns (4) and (8) of Table 1. We now present a brief description of the resonances for each galaxy.

3.3 Resonance structures in the individual galaxies

NGC1097. This nearby SBb galaxy (D = 14.5 Mpc) has a nested bar system, first reported by Buta (1988), and later measured by Wozniak et al. (1995). The two bar radii are

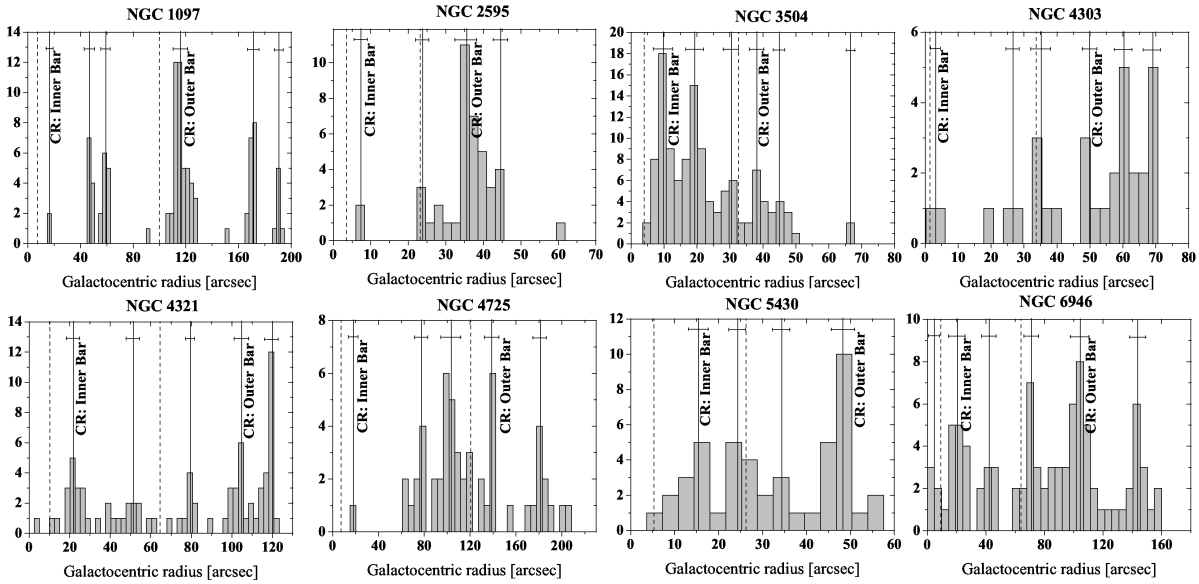

Figure 1. Histograms of the phase reversals as a function of the radial distance, for each galaxy. Ordinate axis shows the number of phase reversals obtained using the residual velocity maps. Dashed vertical lines indicate lengths of nested bars. Solid vertical lines mark the central positions of those peaks identified as resonances; the horizontal segments show the uncertainty in the radius of the resonance.

Table 1. Dynamical parameters of nested bars.

Object NGC	Type	r_{bar}^{in} (arcsec)	r_{CR}^{in} (arcsec)	$\mathcal{R}^{in}$	Ω^{in} (km·s^{-1}·kpc^{-1})	r_{bar}^{out} (arcsec)	r_{CR}^{out} (arcsec)	$\mathcal{R}^{out}$	Ω^{out} (km·s^{-1}·kpc^{-1})	Γ
(1)	(2)	(3)	(4)	(5)	(6)	(7)	(8)	(9)	(10)	(11)
1097	SB(s)b	7.2	16.5±2.7	2.3±0.4	$136.8^{+12.8}_{-9.6}$	98.2±14.4	114.5±7.1	1.1±0.2	$38.3^{+2.3}_{-2.1}$	$3.6^{+0.4}_{-0.3}$
2595	SAB(rs)c	4.2±0.2	8.9±1.2	2.1±0.3	$123.2^{+15.9}_{-12.5}$	23.8±1.0	36.5±2.4	1.5±0.1	$35.1^{+2.4}_{-2.1}$	$3.5^{+0.5}_{-0.4}$
3504	SAB(s)ab	4.1±0.4	9.9±2.7	2.4±0.7	$230.5^{+104.7}_{-59.9}$	33±3	37.6±2.4	1.2±0.1	$67.1^{+3.5}_{-3.3}$	$3.4^{+1.5}_{-0.9}$
4303	SAB(rs)bc	2.1±0.1	4.6±1.0	2.2±0.4	$135.0^{+10.0}_{-8.4}$	33.0±2.6	49.9±1.1	1.5±0.1	$39.0^{+0.7}_{-0.6}$	$3.5^{+0.5}_{-0.4}$
4321	SAB(s)bc	9.7±0.5	20.9±3.3	2.2±0.4	$81.1^{+11.3}_{-8.6}$	72.0±12.0	102.5±3.3	1.4±0.1	$22.8^{+0.7}_{-0.6}$	$3.5^{+0.5}_{-0.4}$
4725	SAB(r)ab	8.2±0.8	17.8±3.8	2.2±0.5	$92.3^{+7.9}_{-6.6}$	123.3±5.2	139.7±3.8	1.2±0.1	$26.7^{+0.7}_{-0.6}$	$3.5^{+0.3}_{-0.3}$
5430	SB(s)b	5.6±0.6	15.2±3.0	2.7±0.8	$79.5^{+17.1}_{-12.4}$	26.1±1.0	47.5±2.6	1.8±0.1	$23.8^{+1.7}_{-1.5}$	$3.3^{+0.8}_{-0.6}$
6946	SAB(rs)cd	9.2±1.2	20.2±4.8	2.2±0.6	$174.9^{+36.7}_{-24.8}$	65±5	102.9±6.6	1.6±0.2	$51.3^{+2.8}_{-2.5}$	$3.4^{+0.7}_{-0.5}$

Column (1): names of objects, Column (2) morphologycal type taken from RC3 (de Vaucouleurs et al. 1991). Column (3) nuclear bar radius (see text for details and references). Columns (4), (5), respectively: corotation radius of nuclear bar from our phase reversals method, and $\mathcal{R}$: ratio of the corotation radius and the bar length. Column (6): pattern speed value associated with bar corotation. Columns (7)-(10): same parameters as columns (3)-(6) but for the large bar. Column (11): values of Γ the ratio between the inner and outer pattern speeds.

given in Table 1 (columns 3, 7). The inner bar length is from Kondo et al. (2012), and from Davis et al. (2009) who argue that the bar length should be less than 8 arcsec. The outer bar length is the mean of the values given in Wozniak et al. (1995), Kondo et al. (2012), Muñoz-Mateos et al. (2013) and Piñol-Ferrer et al. (2014); the associated uncertainty is the standard deviation of these values. The histogram (in Fig. 1) shows six peaks. Peak four, the strongest is assigned to the corotation radius of the main bar using the BC criterion, and we take peak one as corotation of the inner bar. These radii are in Table 1, columns 4 and 8. Our values for the corotation radius of the outer bar (114.5±7.1 arcsec) and its angular rate (38.3±2.2 km·s^{-1}·kpc^{-1}), agree, within the uncertainties, with previous results obtained using different methods (see Table 1, columns 8 and 10). Van de Ven & Fathi (2010), find an angular rate and a corotation radius of and 35 km·s^{-1}·kpc^{-1} and 122.3 arcsec, respectively. Both values are reproduced by Piñol-Ferrer et al. (2014), using a dynamical model for the gravitational potential to determine the main bar pattern speed as 36±2 km·s^{-1}·kpc^{-1}, placing corotation at a deprojected distance of 122.3±7.1 arcsec from the galaxy center. They also apply the Tremaine-Weinberg method to an ionized gas velocity field to calculate the pattern speed, finding a value of 30±8 km·s^{-1}·kpc^{-1}.

NGC2595. This galaxy has a clear double bar. The assumed distance is 58.1 Mpc. Our procedure yields four peaks (Figure 1). Applying the BC criterion peaks 1 and 3 lie at corotation for the inner and outer bar corotation, respectively. The radii of the two bars are estimated by finding the radial position of the maxima in ellipticity at constant position angle for ellipse fitting of the isophotes on a 3.6 μm

image (Spitzer archive), which are deprojected using the PA of the bar and PA and inclination of the disc.

NGC3504. In this barred, ringed galaxy (Buta & Crocker 1993) we find six peaks (Figure 1). We attribute peak 1 to the corotation of the inner bar and peak 4 to that of the outer bar, using the BC criterion. The outer bar length is from Kenney et al. (1993); the semimajor axis of the nuclear bar is determined from the ellipticity and position angle curves of the isophotes as functions of radius. Our pattern speed for the main bar (Ω_P = 67.6 km·s^{-1}·kpc^{-1} with D = 19.8 Mpc) is quite close to Ω_P = 77 km·s^{-1}·kpc^{-1} found by Kenney et al. (1993), but inconsistent with the upper limit $\Omega_P \leqslant 41$ km·s^{-1}·kpc^{-1}, determined by Kuno et al. (2000); this is satisfied only by our outermost resonance at 66.6±1.6 arcsec (see Figure 1) with an angular speed of 37.9±0.9 km·s^{-1}·kpc^{-1}.

NGC 4303 (M61). We find six peaks in the histogram (Figure 1). Using the BC criterion we find corotation for the inner bar and the main bar as peaks 1 and 4, respectively. The inner bar length is the mean of those of Erwin (2004) and Perez-Ramirez et al. (2000), while the outer bar length is the value of Erwin (2004). Koda & Sofue (2006) apply a cloud-orbit model finding a corotation radius of 38.5 arcsec for the main bar, almost compatible with our value (Table 1). Our corotation radius of the nuclear bar (4.6 arcsec) is consistent with the length of the gas bar in Koda & Sofue (2006), and with the analysis of Schinnerer et al. (2002), who argued that it should lie between the inner ILR (at 2 arcsec) and the outer ILR (at 10-14 arcsec) of the outer bar. Egusa et al. (2009) establish a lower limit for the primary bar corotation radius $r_{CR} \geqslant 36$ arcsec (consistent with our result), and estimate the angular speed of the outer bar assuming a distance of 16.1 Mpc, Ω_P = 24±29 km·s^{-1}·kpc^{-1}, compatible with our value given the large uncertainty.

NGC 4321 (M100). This large nearby spiral (D = 15.9 Mpc) is intensively studied. Its inner bar is clearly visible in the near IR (see Knapen et al. (1995)), but its major bar is weak, and rather oval in shape. We find five peaks in our histogram (Figure 1). The BC criterion yields peak 1 as the corotation of the inner bar and peak 4 that of the outer bar. The sizes of the bars are from Erwin (2004), noting also the value by Muñoz-Mateos et al. (2013). The corotation radius for the main bar determined here and its pattern speed (see Table 1) are in agreement with most previous studies which used a wide variety of methods. We have discussed these, for the outer bar only, in Font et al. (2011), to which the reader is referred. Hernandez et al. (2005) used the TW method to determine the pattern speed of the inner bar, finding 48 km·s^{-1}·kpc^{-1} which not unexpectedly using TW on gas for an inner bar, does not coincide with our value.

NGC 4725. This early type ringed galaxy shows a diffuse primary bar with a nested nuclear bar. The phase reversals show five peaks (Figure 1). With the BC criterion we assign peaks 1 and 4 respectively to the corotations of the inner and outer bars. The bar lengths are from Erwin (2004) and Muñoz-Mateos et al. (2013). Buta (1988) found a pattern speed for this galaxy between 13.1-29.5 km·s^{-1}·kpc^{-1}, placing corotation at 186 arcsec. These are not compatible with our values for the outer bar (Table 1), but agree with the outermost resonance in our phase histogram, which we attribute to the spiral structure, and is located at 181.3±4.9 arcsec, with an angular speed of 21.1±0.6 km·s^{-1}·kpc^{-1} (taken a distance of 17.1 Mpc).

NGC 5430. This galkaxy, located at 49.0 Mpc, has a strong outer bar, with asymmetric outer disc, suggesting a recent merger. It shows four histogram peaks. Using the BC criterion we assign peak 1 to the nuclear bar corotation, and peak 2 to that of the outer bar. The length of the nuclear bar is determined as the radius of the local maximum of the ellipticity curve, while the radius of the main bar is calculated by deprojecting the value given in Keel (1987).

NGC6946. Elmegreen et al. (1998) first reported the bar-within-a-bar morphology, analysing near-infrared images of this late-type galaxy. The histogram, within a region of radius 125 arcsec, shows six peaks. Peaks two and five are assigned as corotations of the two bars, using the BC criterion.The outer bar size (Table 1) is an average of the measurements of Regan & Vogel (1995) and of Elmegreen et al. (1998); for the nuclear bar we calculated the mean of the values of Elmegreen et al. (1998) and Tsai et al. (2013). The TW method was applied to CO data by Zimmer et al. (1989) and to Hα data by Fathi et al. (2007). The first authors found a pattern speed of 39±13 km·s^{-1}·kpc^{-1}, which is well reproduced if corotation occurs at the outermost peak (see Figure 1), at 143.63.3 arcsec for which the angular velocity is 39±13 km·s^{-1}·kpc^{-1} (assuming a distance of 5.9 Mpc). Fathi et al. (2007) determine two pattern speeds: a primary one, of 22^{+4}_{-1} km·s^{-1}·kpc^{-1}, at a radius of 304 arcsec (beyond the limits of our data) and a secondary one of 47^{+3}_{-2} km·s^{-1}·kpc^{-1}, which is in agreement, within uncertainties, with the angular rate for the outer bar found here. Values for the corotation radius and pattern speed by authors using other techniques can be found in Fathi et al. (2007).

4 DISCUSSION

We have determined the pattern speeds of the major bar and the nuclear bar in eight galaxies, from early to late types, using emission in Hα from the ionized gas in their interstellar media. The technique is straightforward, but can be performed only with 2d coverage of the velocity field across the whole galaxy disc, with good angular and velocity resolution. This is possible using Fabry-Perot observations as described here, but would be possible using maps of sufficient resolution in HI or CO emission lines. We find in all cases that the nuclear bar is rotating with angular velocity considerably greater than the outer bar, showing that the bars are dynamically decoupled. The range of values for the pattern speed ratio is quite narrow, ranging from 3.3 to 3.6, with a mean value of $3.5^{+0.7}_{-0.5}$. This result is in good agreement with gas models by Englmaier & Shlosman (2004) who predicted a value for this ratio of 3.4 once the inner bar has stabilized its rotation. They showed that before it has achieved this stability the ratio should oscillate between 3.2 and 3.8, which fits surprisingly well the range of values we find here. A series of models in Maciejewski & Athanassoula (2008) predict values for the ratio of bar angular rates between 1.6 and 2.7. We note also that the lowest value for the pattern speed of an inner bar, 79.5 km·s^{-1}·kpc^{-1}, is quite close to the lower limit suggested in Maciejewski & Small (2010) for orbitally stable stellar bars. The ratio between the corotation radius of the outer bar and its length is greater than 1 (Table 1, col-

umn 9), agreeing with simulations by Athanassoula (1992). The values for this ratio agree particularly well with the model predictions of Rautiainen et al. (2008), these authors find that this ratio depends on the morphological type, increasing from early type ($\mathcal{R}$=1.15±0.25) to intermerdiate type ($\mathcal{R}$=1.44±0.29) and late type galxies ($\mathcal{R}$=1.82±0.63). The equivalent ratio for the inner bar (Table 1, column 5) is found to be between 2.1 and 2.7 with a mean of 2.3, agreeing with predictions by Maciejewski & Small (2010).

ACKNOWLEDGMENTS

GHαFaS is a visitor instrument on the William Herschel Telescope, Isaac Newton Group, IAC Observatorio del Roque de los Muchachos, La Palma. We thank Miguel Querejeta for data analysis contributions, Phil James for observations of NGC 4303. J.E.B. thanks APCTP for hospitality at the 7th Korean Astrophysics Workshop; KF thanks the Swedish Research Council and the Swedish Royal Academy of Sciences Crafoord Foundation. Support comes from project AYA2007-67625-CO2-01 of the Spanish Ministry of Science and Innovation, project P3/86 of the Instituto de Astrofsica de Canarias, and the DAGAL network, Marie Curie actions,EU 7th framework programme FP7/2007-2013/REA grant agreement PITN-GA-2011-289313.

REFERENCES

Ann H.B., 2001, AJ, 121, 2515
Athanassoula E., 1992, MNRAS, 259, 345
Buta R., 1988, ApJ Suppl. Ser. 66, 233
Buta R., Crocker D. A., 1993, AJ, 105, 1344
Chemin L. et al., 2006, MNRAS, 366, 812
Contopoulos G., Papayannopulos T., 1980, A&A, 92, 43
Corsini E.M., Debattista V.P., Aguerri J., 2003, ApJ, 599, L29
Daigle O., Carignan C., Amram P., Hernandez O., Chemin L., Balkowski C., Kennicutt R., 2006, MNRAS, 367, 469
Davis R.I., Maciejewski W., Hicks E.K.S., 2009, ApJ, 702,114
de Vaucouleurs G., de Vaucouleurs A., Corwin H. G., Buta R. J., Paturel G., Fouqué P., 1991, Third Reference Catalogue of Bright Galaxies. Springer, New York, NY
Dicaire I. et al., 2008, MNRAS, 385,553
Egusa F., Kohno K., Sofue Y., Nakanishi H., Komugi S., 2009, ApJ, 697, 1870
Elmegreen D.M., Chromey F.R., Santos M., 1998, AJ, 116, 1221
Emsellem E., Fathi K., Wozniak H., Ferruit P., Mundell C.G., Schinnerer E., 2006, MNRAS, 365, 367
Englmaier P., Shlosman I., 2004, ApJ, 617, L115
Epinat B., Amram P., Marcelin M., 2008, MNRAS, 390, 466
Erwin P.E., 2004, A&A, 415, 941
Erwin P.E., 2011, MSAIt, 18, 145
Erwin P.E., Sparke L., 2002, AJ, 124, 65
Fathi K., Toonen S., Falcón-Barroso J., Beckman J.E., Hernandez O., Daigle O., Carignan C., de Zeeuw T., 2007. ApJ, 667, L137
Fathi K., Beckman J.E, Piñol-Ferrer N., Hernandez O., Martínez-Valpuesta I., Carignan C., 2009, ApJ, 704, 1675
Font J., Beckman J.E., Epinat B., Fathi K., Gutiérrez, L., Hernandez O., 2011, ApJ, 741, L14
Font J., Beckman J.E., Querejeta M., Epinat B., James P.A., Blasco-Herrera J., Erroz-FerrerS., Pérez I., 2014, ApJSuppl., 210, 2
Hernandez O., Wozniak H., Carignan C., Amram P., Chemin L., Daigle O., 2005, ApJ, 632, 253
Kalnajs, A.J., 1978, , in IAU symp. No. 77, Structure and properties of nearby galaxies. Ed. E.M. Berkhuijsen and R. Wielebinski (Boston: IAU),113.
Keel W.C., 1987, A&A, 172, 43
Kenney J.D.P., Carlstrom J.E., Young J.S., 1993, ApJ, 418, 687
Kennicutt R. C. et al., 2003, PASP, 115, 928
Knapen J.H., Beckman J.E., Shlosman I., Peletier R.F., Heller C.H., de Jong R.S., 1995, ApJ, 443, L73
Koda J., Sofue Y., 2006, PASJ, 58,299
Kondo T. et al., 2012, ApJ, 751, L18
Kuno N., Nishiyama K., Nakai M., Sorai K., Vila-Vilaró B., Handa T., 2000, PASJ, 52, 775
Maciejewski W., Athanassoula E., 2008, MNRAS, 389, 545
Maciejewski W., Singh H., 2008, in ASP Conference Series, 396, Formation and Evolution of Galaxy Disks, ed. J. Funes and E.M. Corsini (San Francisco, CA: ASP), 317
Maciejewski W., Small E., 2010, ApJ. 719, 622
Maciejewski W., Sparke L., 2000, MNRAS, 313, 745
Muñoz-Mateos et al., 2013, ApJ, 771, 59
Perez-Ramirez, D., Knapen, J.H., Peletier, R.F., Laine S., Doyon R., Nadeau D., 2000, MNRAS, 317, 234
Pfenniger D., Norman C., 1990, ApJ , 363, 391
Piñol-Ferrer N., Fathi K., Carignan C., Font J., Hernandez O., Karlsson R., van de Ven G., 2014, MNRAS, 438, 971
Rautiainen P., Salo H., 1999, A&A, 348, 737
Rautiainen P., Salo H., Laurikainen E., 2002, MNRAS, 337, 1233
Rautiainen P., Salo H., Laurikainen E., 2008, MNRAS, 388, 1803
Regan M. W., Vogel S. N., 1995, ApJ, 452, L21
Schinnerer E., Maciejewski W., Scoville N., Moustakas L.A., 2002, ApJ, 575, 826
Shen J., Debattista V.P., 2009, ApJ., 690, 758
Shlosman I., Frank J., Begelman M.C., 1989, Nature, 338, 45
Surace, C. et al., 2009, in ASP Conference Series, 411, Astronomical Data Analysis Software and Systems XVIII, ed. D. A. Bohlender, D. Durand, and P. Dowler (San Francisco, CA: ASP), 502
Tsai, C. et al., 2013, ApJ, 776,70
Tremaine S., Weinberg MD., 1984, ApJ, 282, L5
Van de Ven G., Fathi K., 2010 ApJ, 723, 767
Wozniak H., Friedli D., Martinet L., Martin P., Bratschi P., 1995, A&A Suppl. Ser., 111, 115
Zimmer P., Rand R.J., McGraw J.T., 2004, ApJ, 607, 285

This paper has been typeset from a TEX/ LATEX file prepared by the author.